

Multiband Description of Optical Conductivity in Ferropnictide Superconductors

O.V. Dolgov · D.V. Efremov · M.M. Korshunov ·
A. Charnukha · A.V. Boris · A.A. Golubov

Received: 2 December 2012 / Accepted: 14 February 2013 / Published online: 22 March 2013
© Springer Science+Business Media New York 2013

Abstract We study optical properties of the multiband superconductors with an s_{\pm} order parameter symmetry. By comparing results of our theory with experimental data on optical conductivity for $\text{Ba}_{0.68}\text{K}_{0.32}\text{Fe}_2\text{As}_2$ single crystals, we show that satisfactory description of the novel superconductors can be obtained only considering a strong electron-boson coupling. We reexamine the effect of disorder and demonstrate that multiband superconductors are more robust with respect to it than naively expected by simple analogy with paramagnetic impurities in single-band superconductors. Moreover, disorder may give rise to new effects, in particular to a phase transition $s_{\pm} \rightarrow s_{++}$. We discuss how the systematic study of disorder impact on the density of states and the optical conductivity may provide information on the underlying order parameter structure.

Keywords Multiband superconductivity · Optical conductivity · Effects of disorder

1 Introduction

The discovery of iron-based superconductors [1] put forward experimental and theoretical efforts to understand the

mechanism of high-temperature superconductivity in these compounds. These studies yielded a comprehensive experimental description of the electronic Fermi surface (FS) structure, which includes multiple FS sheets, in good agreement with density functional calculations [2, 3]. Partial nesting between at least two of these sheets leads to a spin-density-wave (SDW) instability that renders the metallic parent compounds antiferromagnetic.

At finite electron or hole doping, SDW-order changes to superconductivity. In the superconducting phase, due to the proximity to the SDW-state spin fluctuations become the source of strong repulsive interband interactions and might lead to the superconductivity with different signs of the order parameter on distinct FS sheets, the so-called s_{\pm} symmetry [4, 5]. Therefore, one of the important questions in this regard is how strong the electron-boson interaction in these materials. The answer to this question is also necessary since most of the modern theories are constructed in the limit of a weak coupling.

Since varying amounts of disorder are present in Fe-based superconductors (FeSC) and because superconductivity is created in most cases by doping, it is important to understand the role of impurities. It has been shown that in an s_{\pm} state, any nonmagnetic impurity, which scatters *solely* between the bands with a different sign of the order parameter suppresses T_c in the same way as a magnetic impurity in a single band BCS superconductor [6, 7]. Therefore, the critical temperature T_c should obey the Abrikosov–Gor’kov (AG) behavior [8]. However, in several experiments on FeSC, e.g., Zn substitution or proton irradiation, it is found [9–12] that the T_c suppression is much less than expected in the AG theory. It has therefore been suggested that the s_{\pm} state is not realized at all in these systems, and that a more conventional two-band order parameter without sign change (s_{++}) is the more likely ground state [13–15].

O.V. Dolgov (✉) · D.V. Efremov · A. Charnukha · A.V. Boris
Max Planck Institute for Solid State Research, Stuttgart, Germany
e-mail: o.dolgov@fkf.mpg.de

M.M. Korshunov
L.V. Kirensky Institute of Physics, Krasnoyarsk, Russia

M.M. Korshunov
Siberian Federal University, Krasnoyarsk, Russia

A.A. Golubov
Faculty of Science and Technology and MESA+ Institute of
Nanotechnology, Enschede, The Netherlands

Here, we show that the study of the optical conductivity may give answers to all questions mentioned above. The first part is devoted to the theoretical and experimental investigation of the strength of the electron-boson coupling. We develop the model for multiband superconductors that is capable of describing FeSC in the whole range of couplings (from weak to strong). The computed optical conductivity and specific heat were compared with experimental data on the optimally hole-doped compound $\text{Ba}_{0.68}\text{K}_{0.32}\text{Fe}_2\text{As}_2$ (BKFA) that has the highest transition temperature of 38.5 K [16, 17]. This analysis clearly demonstrates that a satisfactory description of the bulk thermodynamical properties in the superconducting state can only be obtained via a strong coupling to spin fluctuations or other bosons with the spectral weight concentrated at 10–20 meV.

The second part of the paper deals with the physical consequences of impurity scattering for isotropic s_{\pm} two-band superconductor within the self-consistent T -matrix approximation for impurity scattering. As it was shown in the recent study [6, 7, 18, 19], s_{\pm} superconductors can be divided into two types with respect to their sensitivity to a disorder. The first type is the one which has been largely discussed so far in the literature, for which T_c is suppressed as disorder is increased until superconductivity vanishes at a critical value of the impurity scattering rate. There is, however, a second type of s_{\pm} superconductor, for which T_c tends to a finite value as disorder increases; at the same time the gap function acquires a uniform sign, i.e., undergoes a transition from s_{\pm} to s_{++} . We identify the peculiarities of behavior of the second type s_{\pm} superconductors as a function of impurity concentration, which may serve as a test of s_{\pm} symmetry of the order parameter.

2 Optical Conductivity of $\text{Ba}_{0.68}\text{K}_{0.32}\text{Fe}_2\text{As}_2$ Single Crystals

The most incisive experimental data have been obtained on high-quality single-crystals of iron pnictides with the so-called 122 structure, for instance on BaFe_2As_2 with K substituted for Ba or Co for Fe resulting in hole and electron dopings, respectively. Five FS sheets have been found in calculations and confirmed by numerous independent experimental studies. In the reduced Brillouin-zone scheme, these are three hole pockets at the Γ point and two almost degenerate electron pockets at the X point with nesting between hole and electron sheets. Optimally hole-doped material $\text{Ba}_{0.68}\text{K}_{0.32}\text{Fe}_2\text{As}_2$ (BKFA) has the transition temperature of 38.5 K. A four-band Eliashberg theory with strong interband coupling has already proven successful in accounting for the transition temperature, as well as the temperature dependence of the free energy and superconducting gaps for

this compound [20]. This analysis has made clear that a satisfactory description of the bulk thermodynamical properties in the superconducting state can only be obtained via a strong coupling to spin fluctuations or other bosons with the spectral weight concentrated near 20 meV.

Here, we use the same formalism to describe the far-infrared optical response of these compounds. The main input of the theory is the spectral functions of the electron-boson interaction $B(\omega)$ (Eliashberg function; analogous to that of the electron-phonon interaction $\alpha^2F(\omega)$). In a four band system, it can be decomposed into 16 functions $B_{ij}(\omega)$, where i and j label the four Fermi surface sheets ($i, j = 1, 2, 3, 4$). The *standard* Eliashberg functions determine superconducting and thermodynamical properties such as the superconducting transition temperature and gaps, electronic specific heat, de Haas-van Alphen mass renormalizations etc., and are defined as

$$B_{ij}(\omega) = \frac{1}{N_i} \sum_{\mathbf{k}, \mathbf{k}', \nu} |g_{\mathbf{k}, \mathbf{k}'}^{ij, \nu}|^2 \delta(\epsilon_{\mathbf{k}}^i) \delta(\epsilon_{\mathbf{k}'}^j) \delta(\omega - \omega_{\mathbf{k}-\mathbf{k}'}^{\nu}), \quad (1)$$

where N_i is the partial density of states per spin on the i 'th FS sheet and $g_{\mathbf{k}, \mathbf{k}'}^{ij}$ is the matrix element of electron-boson interactions. Transport and electrodynamic properties are defined by 16 *transport* Eliashberg functions (which enter the Boltzmann kinetic equation) differ by the kinetic factor $(v_{Fi}^{\alpha}(\mathbf{k}) - v_{Fj}^{\beta}(\mathbf{k}'))^2 / 2 \langle v_{Fi}^{\alpha 2} \rangle$ under summations over \mathbf{k} and \mathbf{k}' . Here, v_{Fi}^{α} is the α 'th Cartesian component of the Fermi velocity on i 'th FS. The average Fermi velocity is related to the plasma frequency by the standard expression $\omega_{pl i}^2 = 8\pi e^2 N_i \langle v_{Fi}^2 \rangle = 8\pi e^2 \sum_{\mathbf{k}} v_{Fi}^2(\mathbf{k}) \delta(\epsilon_{\mathbf{k}}^i)$.

We set the input parameters, namely, the densities of states for hole bands to be $N_1 = 22 \text{ Ry-st}^{-1}$, $N_2 = 25 \text{ Ry-st}^{-1}$, and for electron bands to be $N_3 = N_4 = 7 \text{ Ry-st}^{-1}$. The spectral function of the intermediate boson, was taken following [21] in the form of a spin-fluctuation spectrum $\tilde{B}_{ij}(\Omega) = \lambda_{ij} f(\Omega/\Omega_{sf})$ with a linear Ω -dependence at low frequencies. Here, $f(\Omega)$ is a normalized function, λ_{ij} is the coupling constant corresponding to a pairing between bands i, j , and Ω_{sf} is a characteristic spin-fluctuation frequency. Numerical values of last two quantities correspond to those in [20], $\Omega_{sf} = 13 \text{ meV}$ and

$$\lambda_{ij} = \begin{pmatrix} 0.2 & 0 & -1.7 & -1.7 \\ 0 & 0.2 & -0.25 & -0.25 \\ -5.34 & -0.89 & 0.2 & 0 \\ -5.34 & -0.89 & 0 & 0.2 \end{pmatrix}. \quad (2)$$

Negative (repulsive) elements correspond to the *interband* hole–electron repulsion, while the positive (attractive)—to the *intra-band* attraction.

In order to apply this full 4-band model to description of the transport properties, one has to take into account an additional set of 4 plasma frequencies and a 4x4 matrix of impurity scattering rates. On the other hand, in the case of

BKFA it is known that three larger gaps have approximately the same value $|\Delta_A| \equiv |\Delta_1| \approx |\Delta_3| \approx |\Delta_4| \approx 9$ meV, while the smaller gap is $|\Delta_B| \equiv |\Delta_2| \approx 3$ meV (see [20, 22–25]). These gaps can be identified as a gap on the outer hole-like Fermi surface (Δ_B) and a group of three gaps with a magnitude $\sim \Delta_A$ on the inner hole-like and the two electron-like Fermi surfaces. Minimizing the ground-state energy subject to this grouping constraint yields an effective 2-band model.

The effective 2-band model closely reproduces all the predictions of the 4-band model such as the superconducting transition temperature $T_c = 38.4$ K, superconducting gaps $\Delta_A = 9.7$ meV and $\Delta_B = 3.7$ meV. The calculated densities of states N_A and N_B are very similar, in accordance with the partial Sommerfeld constants obtained from the specific heat data.

Given the boson spectrum centered at 13 meV consistent with the energy of the spin resonance excitation in this material [26],¹ one obtains the following 2-band model coupling matrix: $\lambda_{AA} = 4.36$, $\lambda_{BB} = 0.2$, $\lambda_{AB} = -0.35$, $\lambda_{BA} = -0.5$, with the fractional density of states being $N_A/(N_A + N_B) = 0.59$ [20]. The first effective intraband coupling constant is an order of magnitude larger than the one predicted for the intraband electron-phonon coupling [27]. It does not, however, bear any physical meaning by itself but rather incorporates contributions from *three* different bands. Note that the coupling matrix has been inferred from prior measurements. Only two intraband impurity scattering rates enter as free parameters of the theory in addition to the plasma frequencies of the bands.

We have calculated optical conductivity by generalizing standard theory [28, 29] to the multiband case. The results are shown in Fig. 1b together with the data for BKFA (Fig. 1a). The high-energy anomaly at $14 k_B T_c$ is naturally captured by the model. The fact that only the biggest superconducting gap Δ_A is visible in the optical response of BKFA is explained by a small contribution of band *B* to the overall optical conductivity that is the result of a clean limit in the *B*-band (black curves in Fig. 1b).

3 Impact of Interband Impurities on the Optical Conductivity

In [18], the problem of the non-magnetic disorder in two-band superconductors was reexamined. It was shown within the *T*-matrix approximation, that the suppression of T_c can be described by a single parameter depending on the intraband and interband impurity scattering rates. T_c was shown

¹The feedback of superconductivity on the spin fluctuation spectrum observed by neutron scattering [26, 32] was not considered in our model calculation.

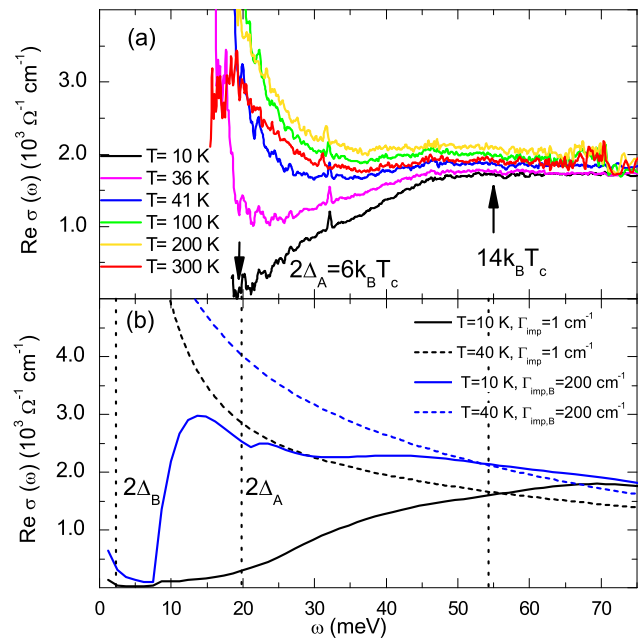


Fig. 1 (a) The real part of the optical conductivity $\sigma(\omega)$ for the single-crystal of optimally doped $\text{Ba}_{0.68}\text{K}_{0.32}\text{Fe}_2\text{As}_2$ at different temperatures. (b) Results of $\text{Re } \sigma(\omega)$ calculations via the Eliashberg formalism for clean bands (black lines), as well as the dirty *B*-band (blue lines) in the superconducting and normal states (Color figure online)

to be more robust against non-magnetic impurities than would be predicted in the trivial extension of the AG theory. A disorder-induced transition from the s_{\pm} state to a gapless and then to a fully gapped s_{++} state was found, controlled by a single parameter—the sign of the average coupling constant. Importantly, it was shown that the gapless state is realized near the transition that should manifest itself in various thermodynamic and transport characteristics. Here, we study the manifestation of this transition in optical conductivity. In Fig. 2, we shows the results of σ_1 calculations for different amount of disorder. It is clearly seen that in the vicinity of transition from the s_{\pm} to s_{++} state, the conventional Drude-response characteristic for a normal metal-state is realized. The origin of this effect is gapless nature of superconductivity near the impurity-induced $s_{\pm} \rightarrow s_{++}$ transition. With further increase of the impurity scattering rate, the optical conductivity changes back from Drude-like to gapped type, but with smaller gap. This behavior is strikingly different from that for superconductors with s_{++} order parameter, where values of two gapes tends to merge at the limit of infinite impurity scattering rate. This type of behavior can be found in MgB_2 [30, 31]. This reentrant behavior of optical conductivity with concentration of nonmagnetic impurities may serve as unambiguous indication for the s_{\pm} order parameter symmetry.

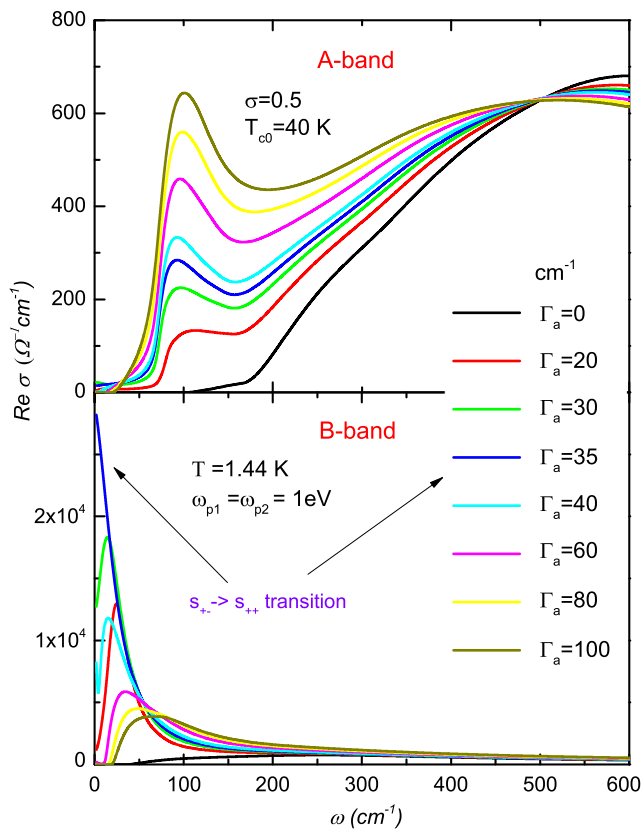


Fig. 2 Real part of the optical conductivity $\sigma_1(\omega)$ for different values of the impurity scattering strength. The parameters are: $\sigma = 0.5$, $\beta = 1$, $T = 1.4$ K. The definitions of parameters σ and β are given in [18]

4 Conclusion

We have shown that a qualitative description of the far-infrared optical conductivity for $\text{Ba}_{0.68}\text{K}_{0.32}\text{Fe}_2\text{As}_2$ can be obtained in the framework of an effective two-band Eliashberg theory with a strong coupling to spin fluctuations that is deduced from its four-band counterpart. The linear increase of absorption above the larger superconducting gap can only be observed when the effective band is extremely clean. The interband impurity scattering may cause reentrant behavior of the optical conductivity. This effect may give information about the structure of the underlying order parameter.

Acknowledgements The authors are grateful to B. Keimer, S.-L. Drechsler, P. Fulde, I.I. Mazin, V. Mishra, and D.J. Scalapino for useful discussions. The present work was partially supported by the DFG Priority Programme SPP1458 (DVE, AB, AC), Dutch FOM (AAG), Presidium of RAS program “Quantum physics of condensed matter” N 20.7, Grant “Leading scientific schools of Russia” (NSh 1044-2012.2), RFBR (Grant No. 09-02-00127), Integration Grant of SBRAS-UrBRAS N 44, Russian FCP (GK 16.740.12.0731), and Siberian Federal University (Theme N F-11), The Dynasty Foundation and ICFPM (MMK).

References

1. Kamihara, Y., et al.: J. Am. Chem. Soc. **130**, 3296 (2008)
2. Paglione, J., Greene, R.L.: Nat. Phys. **6**, 645 (2010)
3. Johnston, D.C.: Adv. Phys. **59**, 803 (2010)
4. Mazin, I.I.: Nature **464**, 183 (2010)
5. Hirschfeld, P.J., Korshunov, M.M., Mazin, I.I.: Rep. Prog. Phys. **74**, 124508 (2011)
6. Golubov, A.A., Mazin, I.I.: Phys. Rev. B **55**, 15146 (1997)
7. Golubov, A.A., Mazin, I.I.: Physica C **243**, 153 (1995)
8. Abrikosov, A.A., Gor'kov, L.P.: Sov. Phys. JETP **12**, 1243 (1961)
9. Cheng, P., et al.: Phys. Rev. B **81**, 174529 (2010)
10. Li, Y., et al.: New J. Phys. **12**, 083008 (2010)
11. Nakajima, Y., et al.: Phys. Rev. B **82**, 220504(R) (2010)
12. Tropeano, M., et al.: Phys. Rev. B **81**, 184504 (2010)
13. Kontani, H., Onari, S.: Phys. Rev. Lett. **104**, 157001 (2010)
14. Onari, S., Kontani, H.: Phys. Rev. Lett. **103**, 177001 (2009)
15. Bang, Y., Choi, H.-Y., Won, H.: Phys. Rev. B **79**, 054529 (2009)
16. Charnukha, A., et al.: Phys. Rev. B **84**, 174511 (2011)
17. Golubov, A.A., et al.: JETP Lett. **94**, 333 (2011)
18. Efremov, D.V., et al.: Phys. Rev. B **84**, 180512(R) (2011)
19. Efremov, D.V., et al.: New J. Phys. **15**, 013002 (2013)
20. Popovich, P., et al.: Phys. Rev. Lett. **105**, 027003 (2010)
21. Parker, D., et al.: Phys. Rev. B **78**, 134524 (2008)
22. Evtushinsky, D.V., et al.: Phys. Rev. B **79**, 054517 (2009)
23. Zhang, Y., et al.: Phys. Rev. Lett. **105**, 117003 (2010)
24. Nakayama, K., et al.: Phys. Rev. B **83**, 020501 (2011)
25. Shan, L., et al.: Phys. Rev. B **83**, 060510 (2011)
26. Christianson, A.D., et al.: Nature **456**, 930 (2008)
27. Boeri, L., Dolgov, O.V., Golubov, A.A.: Phys. Rev. Lett. **101**, 026403 (2008)
28. Nam, S.B.: Phys. Rev. **156**, 470 (1967)
29. Shulga, S.V., Dolgov, O.V., Maksimov, E.G.: Physica C **178**, 266 (1991)
30. Mazin, I.I., et al.: Phys. Rev. Lett. **89**, 107002 (2002)
31. Kortus, J., et al.: Phys. Rev. Lett. **94**, 027002 (2005)
32. Inosov, D.S., et al.: Nat. Phys. **6**, 178 (2009)